

Role of Radial Electric Field Shear at the Magnetic Island in the Transport of Plasmas

IDA K., OHYABU N., MORISAKI T., NAGAYAMA Y., INAGAKI S., YOKOYAMA M., ITOH K.,
YOSHIMURA M., LIANG Y., NARIHARA K., KOSTRIOUKOV A. Yu., PETERSON B.J.,
TANAKA K., TOKUZAWA T., KAWAHATA K., SUZUKI H., KOMORI A.
and LHD Experimental Group

National Institute for Fusion Science, Toki 509-5292, Japan

(Received: 21 December 2001 / Accepted: 2 May 2002)

Abstract

The structures of radial electric field and transport at the magnetic island are investigated using $n/m=1/1$ external perturbation coils in the Large Helical Device (LHD). The radial profiles of plasma potential, as well as the electron temperature and density, shows flattening inside the magnetic island and the large shear of the radial electric field is observed at the boundary of the magnetic island. When the current of $n/m=1/1$ external perturbation coils becomes large enough, the finite radial electric field appears inside the magnetic island. The abrupt appearance of plasma flow inside the magnetic island suggests the non-linearity of the viscous force at the boundary of the magnetic island. The thermal diffusivity perpendicular to the magnetic field inside the magnetic island is estimated with the cold pulse propagation, which is produced by a tracer-encapsulated solid pellet (TESPEL). The time delay and amplitude of the electron temperature of the cold pulse show much lower thermal diffusivity inside the magnetic island ($0.16 \text{ m}^2/\text{s}$) than that outside the magnetic island ($2 \text{ m}^2/\text{s}$), which is a clear evidence for the significant reduction of heat transport inside the magnetic island.

Keywords:

radial electric field, magnetic island, spontaneous poloidal flow, flow shear, transport

1. Introduction

The transport at the magnetic island has been recognized to be important, since the phenomena imply a significant change of transport at a rational surface. The recent observations of the internal transport barriers at or near the rational magnetic surface in tokamak plasmas imply the importance of magnetic islands in the plasma confinement [1]. The position of transport barrier is often correlated to the location of low order rational magnetic surface [2]. Since the radial electric field shear is considered to cause or trigger the formation of the transport barrier, the radial electric field shear at the boundary of magnetic island is one of the

candidates to explain the correlation. However, there are few experiments in studying the radial structure of radial electric field at the magnetic island [3,4], because the rotations of magnetic island itself makes the measurements of radial electric field difficult.

There have been the observations that demonstrate the low particle and heat diffusivity inside the magnetic island. The low particle diffusivity inside the magnetic island was observed when the particle is fueled into the magnetic island by fueling pellet, which was called as "snake" modulation, in JET [5]. More recently the possible role of magnetic island on the local variation of

Corresponding author's e-mail: ida@nifs.ac.jp

thermal diffusivity has been reported by RTP experiment [6]. In spite of the importance of transport at the magnetic island, there is no direct measurement of thermal diffusivity inside the magnetic island. This is because, the transport analysis based on the temperature gradient and radial heat flux in the steady state is invalid due to the flattening of electron temperature inside the magnetic island [7]. The localized flattening of the electron temperature profile is due to a modification of the magnetic topology resulting from the magnetic island produced by the perturbation field and not due to the increase of energy transport. When there is no local heating inside the magnetic island, the electron temperature profile shows flattening even though the magnitude of the thermal diffusivity is small inside the magnetic island. In order to evaluate the transport inside the magnetic island, the transient transport analysis is necessary.

Although the structure of radial electric field and radial electric field shear is a crucial parameter to understand the good confinement (low diffusivity) inside the magnetic island, there have been no clear measurements of poloidal flow or radial electric field and transport inside the magnetic island except for plasma edge. The structure of radial electric field and heat transport inside the magnetic island are discussed in this paper.

2. Magnetic Island Produced by the $n/m=1/1$ Perturbation Coil

The Large Helical Device (LHD) [8] is a Heliotron device (poloidal period number $L = 2$, and toroidal period number $M = 10$) with a major radius of $R_{ax} = 3.5 - 4.1$ m, an average minor radius of 0.6 m, magnetic field up to 3 T. The radial electric field (E_r) is derived from the poloidal and toroidal rotation velocity and pressure gradient of Neon impurity measured with charge exchange spectroscopy [9] at the mid plane in LHD (vertically elongated cross section) using a radial force balance. The radial force balance equation can be expressed as $E_r = (en_i Z_i)^{-1} (\partial p_i / \partial r) - (v_\theta B_\phi - v_\phi B_\theta)$, where B_ϕ and B_θ are toroidal and poloidal magnetic field and Z_i , n_i , p_i are ion charge, density and pressure of impurity measured, respectively. The Large Helical Device (LHD) has $n/m=1/1$ external perturbation coils. The size of magnetic island can be controlled up to 10cm by changing the current of the perturbation coils. The spatial resolution of the measurements of the radial electric field using the charge exchange spectroscopy is determined by the length of integration of the signal

along the line of sight within the beam width of the neutral beam. The spatial resolution becomes poor near the plasma center and relatively good near the plasma edge and it is ± 1.5 cm at the $R=4.05$ m.

Figure 1 shows the poloidal cross section of the last closed magnetic flux surface and magnetic island calculated (without zero beta) for the discharge with the $n/m=1/1$ external perturbation coil current, $I_{n/m=1/1}$, of -1200 A and electron temperature and density profiles. The magnetic island is located near the plasma edge at $\rho = 0.85$. As seen in Fig. 1(b), the flattening of both of

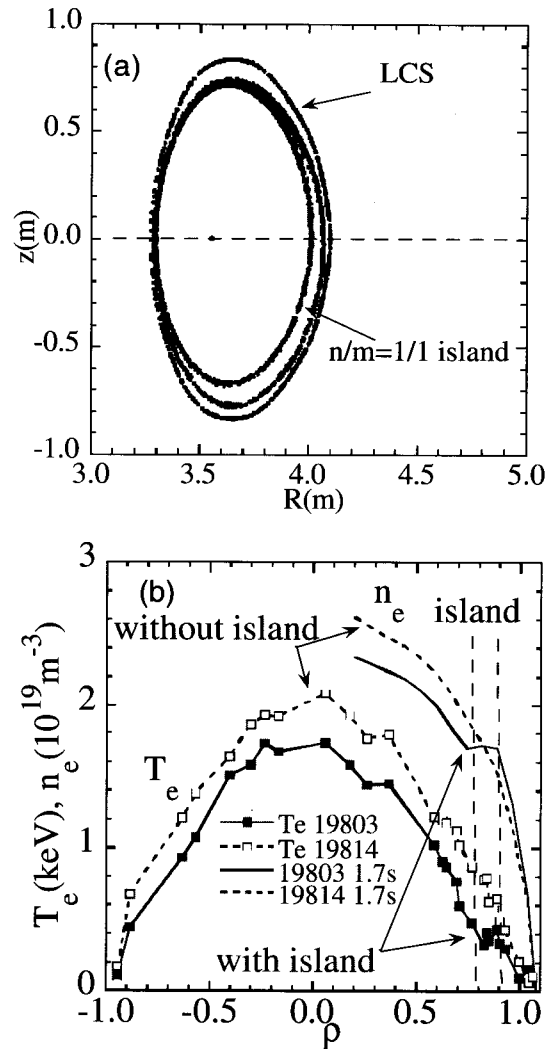


Fig. 1 (a) Poloidal cross section of the last closed magnetic flux surface (LCS) and $n/m=1/1$ magnetic island and (b) radial profiles of electron density and temperature for the plasma with and without magnetic island, where ρ is a normalized minor radius.

electron density and temperature is observed for the plasma with magnetic island ($I_{n/m=1/1} = -1200$ A), while there is no flattening observed for the plasma without magnetic island. The flattening width of electron temperature is considered to represent the width of magnetic island in the plasma, which would not be identical to the width of vacuum magnetic island due to the healing effect [7]. Since there is no pressure gradient inside the magnetic island, one can expect the flat space potential and zero radial electric field inside the magnetic island.

3. Radial Electric Field Profiles Near the Magnetic Island

When the current of $n/m=1/1$ external perturbation coils is small (see 260 A in Fig. 2), no island structure appears in the profile of radial electric field as well as ion temperature. As the perturbation coil current increases, clear structure of magnetic island appears in the radial electric field. Widths of island, W_{Ti} and W_{Er} , are estimated from the radial profiles of ion temperature and radial electric field measured.

The widths are given by a least-squares fit of the measured profiles to the model profiles, where the ion temperature gradient is zero for $R_i - (1/2)W_{Ti} < R < R_i + (1/2)W_{Ti}$ and the radial electric field is zero for $R_i - (1/2)W_{Er} < R < R_i + (1/2)W_{Er}$. Here R_i is the major radius for the center of the magnetic island. Although those widths are not identical because of the difference of radial diffusion of energy and momentum, both widths increase as the current of $n/m=1/1$ external perturbation coils $I_{n/m=1/1}$ is increased. When the size of magnetic island is large (e.g. $I_{n/m=1/1} = -1200$ A) enough to drive the convective flow inside the magnetic island, only the width W_{Ti} , not W_{Er} , can be experimentally determined.

As the perturbation coil current increases, the width of magnetic island estimated from the radial profiles of radial electric field also increases up to 9 cm, which corresponds to 17 % of the averaged minor radius. Here we assume the zero radial electric field inside the magnetic island to estimate the width of island. In the calculation of model profiles, the smoothing due to the spatial resolution of the measurements is taken into account. Because of this smoothing, the apparent radial electric field inside the magnetic island can be finite even the radial electric field is zero as assumed in the model when the width of the island is smaller than the spatial resolution.

In the model, radial electric field jumps at the boundary of magnetic island, i.e. finite values outside

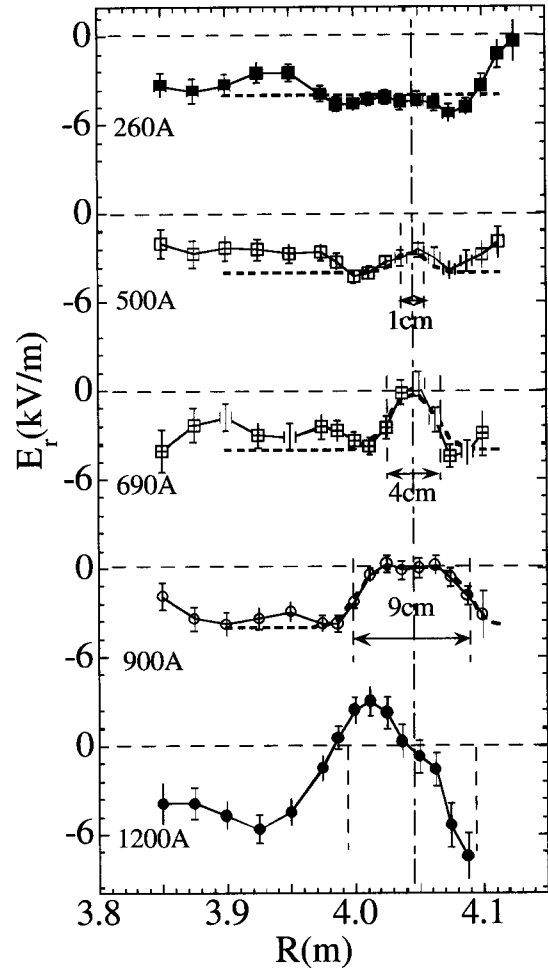


Fig. 2 Radial profiles of radial electric field, measured with charge exchange spectroscopy for various current of $n/m=1/1$ external perturbation coils, $I_{n/m=1/1}$, for the plasma with magnetic field of 1.5 T, vacuum magnetic axis of 3.5 m. The last closed surface are at $R=3.28$ m and $R=4.10$ m at the cross section vertically elongated. The major radius for the center of island, R_i , is indicated with line as a reference. The dashed lines are calculated profiles of radial electric field using simple model, where the radial electric field is zero inside the island. The width of magnetic island, W_{Er} , estimated from radial electric field profiles are also indicated.

the magnetic island and zero radial electric field inside the island. Due to the shear viscosity, the boundary itself should have finite width Δ . This width is determined by the viscous coefficient μ and the ratio of radial electric field to radial current and given by the $\Delta = \sqrt{\mu \epsilon_0 \epsilon_{\text{perp}} E_r / j_r}$, where $\epsilon_0 \epsilon_{\text{perp}}$ is dielectric constant and E_r, j_r are radial electric field and neoclassical radial current to sustain the E_r outside of the magnetic island,

respectively [10]. The values of shear width Δ can be estimated to be 1.2 cm using the experimental values of $\epsilon_0 \epsilon_{\text{perp}} E_r / j_r = 70 \mu\text{s}$ [11] and $\mu = 2 \text{ m}^2/\text{s}$ [12] and it is too small to be measured with the charge exchange spectroscopy which has the spatial resolution of $\pm 1.5 \text{ cm}$.

4. Plasma Space Potential in the Electron and Ion Root

If the space potential is not flat inside the magnetic island, both the radial electric field and the poloidal flow should be finite inside the magnetic island. Because of the conservation of particle flux inside the magnetic island, the poloidal flow should be convective, if it exists inside the magnetic island. When the poloidal flow is convective, the sign of radial electric field should be reversed across the center of magnetic island and radial electric field shear appears inside the magnetic island.

Because of the plasma flow damps (when the island width is below the critical value, 9 cm for the experimental conditions shown in Fig. 2), the radial electric field becomes zero and space potential becomes flat zero inside the magnetic island. Figure 3(a) shows the space potential profiles for the plasma with different magnitude of $n/m=1/1$ perturbation coil current. In LHD, the flattening width of space potential can be extended up to 8 cm, without the appearance of plasma flow along the magnetic flux surface inside the magnetic island. However, when the width of magnetic island exceeds 9 cm (e.g. in the plasma for $I_{n/m=1/1} = -1200 \text{ A}$ in Fig. 2), the plasma flow along the magnetic flux surface inside the island appears as seen in Fig. 3(b). The convective poloidal flow inside the magnetic island is driven by the unbalance of viscous force between inside and outside the magnetic island. If there is no difference of poloidal flow velocity between the two boundaries of magnetic island, the force due to the viscosity at the boundary cancels each other and there should be no net torque to drive the flow inside the magnetic island. When the difference in poloidal torque at the boundaries overcomes the damping of flow inside the magnetic island, the flow along the magnetic flux surface appears inside the magnetic island and the direction of the flow is considered to be determined by the sign of velocity shear at the x-point of magnetic island. The existence of the critical width for the appearance of plasma flow is due to the non-linearity of the viscous force at the boundary of the magnetic island. If the viscous force at the boundary of the magnetic

island is linearly proportional to the flow shear and constant in space, the plasma flow inside the magnetic island is proportional to the square of island width, W , as $v = (W^2/4\delta)(dV_\phi/dr)$, where δ is the shear width at the boundary of magnetic island. Therefore non-linearity of viscous force is required to cause the sudden appearance of plasma flow inside the magnetic island.

When the normalized collisionality of the plasma is high ($\nu_e > 0.1$), the plasma is in the ion root, where the radial electric field is negative and more negative towards the plasma edge [13]. On the other hand, when the normalized collisionality of the plasma is below the critical values of 0.1 ($\nu_e < 0.1$), the plasma is in the

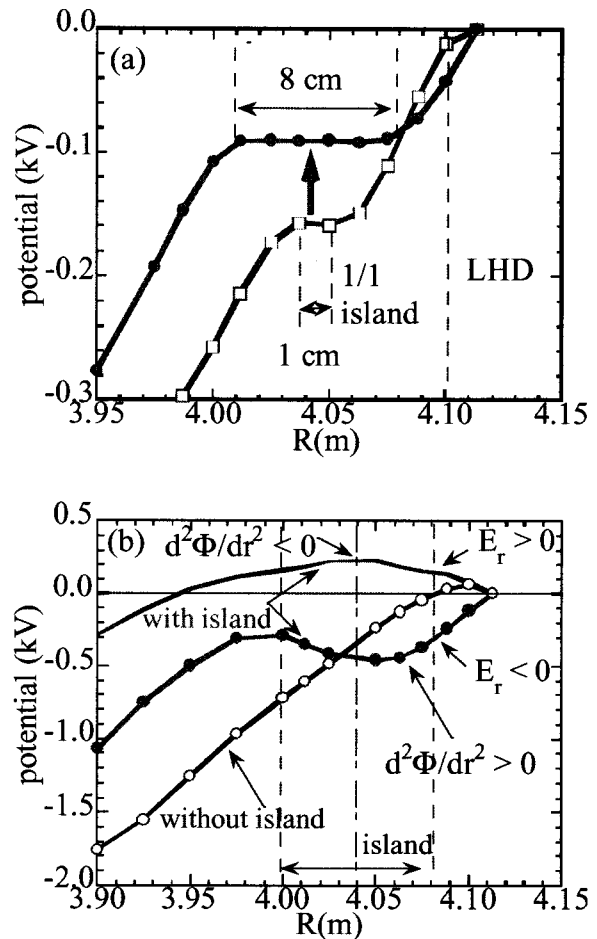


Fig. 3 (a) Radial profiles of space potential for different size of magnetic island. The island width is below the critical values for the sudden appearance of plasma flow inside the magnetic island. (b) Radial profiles of space potential with and without magnetic island for the plasma in the ion root ($\nu_e^* > 0.1$, negative E_r) and electron root ($\nu_e^* < 0.1$ positive E_r).

electron root, where the radial electric field is positive and more positive towards the plasma edge. Therefore the direction of convective poloidal flow should be reversed depending on the sign of edge radial electric field. The change of sign of poloidal flow and the resulting change of curvature of space potential ($d^2\Phi/dr^2 > 0$ or $d^2\Phi/dr^2 < 0$) are clearly observed as seen in Fig. 3. The convective poloidal flow inside the magnetic island is in the direction to decrease of the gap of poloidal flow or radial electric field at the boundary of magnetic island.

5. Transport Inside the Magnetic Island

It is an interesting issue whether the transport is improved or not inside the magnetic island due to the radial electric field. Unless there is a localized fueling or heating at the center of O-point of the magnetic island by pellet injection or ECH, significant peaking of density of temperature is not expected, because magnetic field in the both side of center of magnetic island is connected. The flat profile does not represent the large diffusion or large diffusivity inside the magnetic island. The alternative approach to study the transport is pulse propagation experiment. The transport coefficients such as thermal diffusivity can be estimated from the amplitude and time delay of the heat or cold pulse. The tracer-encapsulated solid pellet (TESPEL) is injected to the X-points of the magnetic island and the cold pulse propagation in the electron temperature is

measured with ECE.

As shown in Fig. 4, the response time of the cold pulse inside the magnetic island is much longer than that observed outside of the magnetic island. The amplitude of the cold pulse is also smaller inside the magnetic island than outside of the island. The time delay and amplitude of the electron temperature of the cold pulse inside the magnetic island is reproduced by simulation of the cold pulse propagation in a slab model with a low thermal diffusivity of $0.16 \text{ m}^2/\text{s}$, which is smaller than that ($2 \text{ m}^2/\text{s}$) outside the magnetic island by more than one order of magnitude. Because the structure of the magnetic island (the effect of poloidal asymmetry) is not included in the analysis, the estimate of the absolute value of the thermal diffusivity is rather crude. However, the differences in pulse propagation inside and outside the magnetic island clearly demonstrate the reduction of energy transport inside the magnetic island.

6. Conclusions

The radial profiles of plasma potential, as well as the electron temperature and density, show flattening inside the magnetic island and the large shear of the radial electric field is observed at the boundary of the magnetic island. When the current of $n/m=1/1$ external perturbation coils becomes large enough, the finite radial electric field appears inside the magnetic island. The plasma flow inside the magnetic island abruptly appears by the non-linearity of the viscous force at the boundary of the magnetic island. The thermal diffusivity perpendicular to the magnetic field inside the magnetic island is estimated with the cold pulse propagation. The thermal diffusivity inside the magnetic island is $0.16 \text{ m}^2/\text{s}$, which is much smaller than that outside the magnetic island ($2 \text{ m}^2/\text{s}$). The experimental results show a clear evidence for the significant reduction of heat transport inside the magnetic island.

This work is partly supported by grant-in-Aid for scientific research of MEXT Japan. The authors would like to thank Dr. A. Fujisawa and Dr. M. Tanaka for useful discussions and the technical support on LHD for the experiments. One of the authors (KI) acknowledged discussion with Prof S-I. Itoh and Dr. M. Yagi.

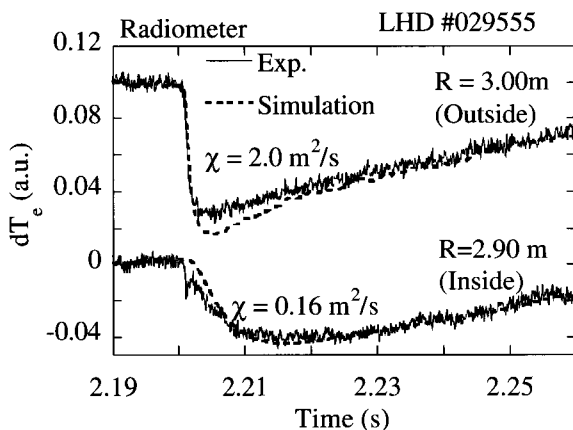


Fig. 4 The response of electron temperature to the cold pulse produced by the tracer-encapsulated solid pellet (TESPEL) inside ($R=2.9 \text{ m}$) the outside ($R=3.0 \text{ m}$) the magnetic island. The calculated time traces reproducing the measurements with the heat diffusivity of $\chi=0.16$ and $2.0 \text{ m}^2/\text{s}$ are also plotted in dashed lines.

References

- [1] Y. Kamada, Plasma Phys. Control. Fusion **42**, A65 (2000).
- [2] P. Mantica *et al.*, Phys. Rev. Lett. **82**, 5048 (1999).
- [3] C. Hidalgo *et al.*, Plasma Phys. Control. Fusion **42**, A153 (2000).

- [4] K. Ida *et al.*, Phys. Rev. Lett. **88**, 015002 (2002).
- [5] A. Weller, A.D. Cheetham, A.W. Edwards, R.D. Gill, A. Gondhalekar, R.S. Granetz, J. Snipes and J.A. Wesson, Phys. Rev. Lett. **59**, 2303 (1987).
- [6] N.J. Lopes Cardozo *et al.*, Phys. Rev. Lett. **73**, 256 (1994).
- [7] Narihara *et al.*, Phys. Rev. Lett. **87**, 135002 (2001).
- [8] M. Fujiwara *et al.*, Nucl. Fusion **40**, 1157 (2000).
- [9] K. Ida, S. Kado and Y. Liang, Rev. Sci. Instrum **71**, 2360 (2000).
- [10] A. Fujisawa *et al.*, Phys. Plasmas **82**, 2669 (1999).
- [11] A. Fujisawa, Plasma Phys. Control. Fusion **41**, A561 (1999).
- [12] H. Yamada *et al.*, Phys. Rev. Lett. **84**, 1216 (2000).
- [13] K. Ida *et al.*, Phys. Rev. Lett. **86**, 5297 (2001).